

IDŐJÁRÁS

Quarterly Journal of the HungaroMet Hungarian Meteorological Service
Vol. 129, No. 2, April – June, 2025, pp. 177–191

Examination of ERA5 thermodynamic profiles and hodographs in the pre-storm environment of severe thunderstorms producing large hail in Hungary between 2019 and 2023

Kornél Komjáti^{*,1,2,3}, Kálmán Csirmaz^{1,3}, and Hajnalka Breuer²

¹*HungaroMet Hungarian Meteorological Service,
Budapest H-1024, Kitaibel Pál u. 1, Hungary*

²*ELTE Eötvös Loránd University Institute of Geography and Earth Sciences
Department of Meteorology,
Budapest H-1117, Pázmány Péter sétány 1/A, Hungary*

³*Hungarian Association of Stormchasers and Storm Damage Surveyors
Budapest H-1139, Fiastyúk u. 57. 3/3., Hungary*

**Corresponding Author email: komjati.k@met.hu*

(Manuscript received in final form June24, 2024)

Abstract— Validated hail observations are available from the hail suppression system operated by the National Chamber of Agriculture since 2019. Using this dataset, large hail (larger than a walnut) reports were collected from recent years. The environments of hail-producing thunderstorms were reconstructed upon ERA5 reanalysis data, and characteristics were sought between thermodynamic profiles and hodographs that could help recognize the environmental conditions for potentially large hail-producing thunderstorms. During the investigation, 52 cases over a total of 35 days were examined. Although the number of cases did not allow for statistical conclusions, the authors identified similarities among the cases through ensemble sounding and hodograph analysis, which could serve as useful operational tools for forecasters.

Key-words: large hail, sounding, hodograph, supercell

1. Introduction

In Europe and globally, large hail causes significant damage every year (Changnon *et al.*, 2009; Allen *et al.*, 2020; Taszarek *et al.*, 2020), and has a serious economic impact, as well (Púčik *et al.*, 2019). Recent research indicates a growing trend in the occurrence of large hail both in the United States and in Europe (Battaglioli *et al.*, 2023). However, it is difficult to establish global criteria for the environmental conditions necessary for the formation of large hail due to the strong influence of mesoscale processes unique to a region (i.e., low-level jet shear-initiated tornado formation is rare in Europe, due to topography) (Taszarek *et al.*, 2023a).

Investigating the conditions for the formation of large hail poses a significant challenge, as models are limited by microphysical schemes, even in high-resolution simulations (Dennis and Kumjian, 2017; Martius *et al.*, 2018; Raupach *et al.*, 2021). Nevertheless, some features as indicators for large hail have been recognized in past studies. Large near-surface storm-relative inflow contributes to the development of wider updrafts (Peters *et al.*, 2019, 2020), promoting longer residence times of hailstones, although excessively strong storm-relative winds can also be detrimental to hail growth (Kumjian and Lombardo, 2020; Kumjian *et al.*, 2023). Furthermore, the examination of storm-relative hodographs has come to the forefront, namely a straighter hodograph can indicate more prolific hail production in supercells (Kumjian *et al.*, 2021; Nixon and Allen, 2022). However, only from kinematic properties, it cannot be determined whether there is potential for large hail; a proper balance of instability, shear, and relative humidity is needed for their formation (Nixon *et al.*, 2023). Analyzing major hailstorm events in Europe between 2021 and 2022, it was found that it is important for about 65% of CAPE to be positioned below the $-10\text{ }^{\circ}\text{C}$ layer, and these events were also characterized by relatively straight shear profile: sharp wind shift in the inflow layer, and straight, elongated hodograph shape between 1 and 3 km (Púčik *et al.*, 2023a). Furthermore, it was found that cell mergers (Wurman *et al.*, 2007; Komjáti *et al.*, 2023; Púčik *et al.*, 2023a, 2023b; Piasecki *et al.*, 2023) and boundary interactions can also intensify storm severity (Maddox *et al.*, 1980, Markowski *et al.*, 1998, Magee and Davenport, 2020; Púčik *et al.*, 2023b). Numerous researches have shown in the past decades that severe hailstorms occur regularly in the Carpathian Basin, these are based on either observations (Horváth and Geresdi, 2001; 2003) or model simulations (Horváth *et al.*, 2006; 2009; Csirmaz, 2015). All of these studies relate the largest hailstone events to supercell convection but did not provide approaches to assess the specific atmospheric background conditions necessary for very large hail which could then be applied in the operational forecasting workflow.

In this paper, we selected cases characterized by observed damaging hail (walnuts or eggs-sized hail, these categories cover the size range above 3 cm) recorded in the National Chamber of Agriculture (NAK) hail observation

database. Ensemble thermodynamic diagrams and hodographs were prepared using ERA5 reanalysis data provided by the ECMWF (European Centre for Medium-Range Weather Forecasts) integrated forecast system. Despite the relatively small number of cases, distinctive patterns are discernible, which confirm the conclusions based mostly on previous numerical simulation studies presented above. The results are detailed in Section 3.

2. Methodology

For the analysis, we relied on the hail observation data from the NAK, which were reported by generator operators of the hail suppression system, specifying the size of fallen hailstones (wheat, pea, cherry, walnut, egg-sized hail) and the location of each observation (longitude and latitude of the town where the observation took place). The system has been operational in Hungary since 2018, and meteorologist-validated data (hail observations compared against radar data) have been available at HungaroMet since 2019. In this study, we examined weather events where damaging hail has fallen. For this, we analyzed cases falling into the top two categories of the available size-category system (walnuts and eggs-sized hail). These two sizes of hail were uniformly called large hail in this study. The observation period spanned from the 15th of April to the 30th of September every year, and we considered a five-year interval which yielded a total of 35 days characterized by large hail size. Naturally, multiple hail observations were associated with a given day, resulting in a total of 52 cases available for analysis. The authors considered that if there were several large hail observations on a given day (which may also result from the inconsistency of the detection system), then the environment associated with each observation should be examined. As a result, those weather situations where several large hail-producing cells have formed dominate the statistics to an extent in this study. ERA5 data were used for the investigation, namely, to find qualitative relationships between the background conditions provided by the dataset and the hail size produced by storms formed in these environments. The ERA5 reanalyses, according to research in recent years, are considered as one of the most reliable reanalysis datasets (*Li et al.*, 2020; *Taszarek et al.*, 2020, 2021; *Coffer et al.*, 2020), and developed by the ECMWF is available from 1940 to the present, with an hourly frequency, a horizontal grid resolution of $0.25^\circ \times 0.25^\circ$ degrees, and a total of 137 model levels.

Data selection was based on ERA5 grid points closest to observation sites, and the time was chosen to be the nearest hour preceding the observation, thus representing a possible environment for storms producing large hail. Python programs were developed to process the data, and the SHARPPy (v1.4.0b1) software was applied for displaying soundings and hodographs (*Blumberg et al.*, 2017). A composite hodograph was also created from the u and v wind

components of ERA5 data, using the 75th percentiles of the datasets at each given level in order to examine the vertical wind profile from a storm-relative perspective. For visualization, the Sam Brandt Hodograph Plotter [1 – GitHub] was utilized, and a relative vertical wind profile was created for the right-moving cell (conclusions drawn from left-moving cells were similar). To determine the storm-relative winds, we shifted the coordinate system to the endpoint of the storm motion vector. Consequently, this location became the reference point (origin), rendering the storm motion vector to be represented as 0. From this point, we recalculated the environmental winds for creating the storm-relative hodograph.

In order to confirm the results extracted from 52 cases, we evaluated them in six additional case studies. Among these six cases, we provide a more detailed presentation of June 12, 2018 (Section 3.3), with the results from the other 5 cases presented in the Appendix section (Appendix A1-A5). ERA5 data were obtained from the nearest grid point to these observations, and displayed on the rawinsonde.com website [2 – Rawinsonde] (Taszarek *et al.*, 2023b).

3. Results

3.1. Ensemble of ERA5 sounding

Having examined the ensemble of sounding data, we found some characteristics that may generally promote the formation of large hail (*Fig. 1*). Our first observation was that in the near-surface layer (up to approximately 850 hPa), the ensemble of the analysis profiles exhibited greater spread, indicating that large hail-producing thunderstorms can also occur in a relatively drier environment near the surface as opposed to the expected relatively moist environment. The mean dewpoint deficit on the lowest level was 6.3 °C, and the 75th percentile of the dewpoint deficit was 9.4 °C. In drier cases, only air parcels driven by strong forcing mechanisms could reach the lifting condensation level, thereby promoting the formation of fewer but more intense cells with wider updrafts (Mulholland *et al.*, 2021). Secondly, in this layer (particularly in the lower few hundred meters), northerly winds dominated in most cases, which could have facilitated surface drying. Our next observation was that between 850 and 700 hPa (at the approximate top of the inflow layer – Thompson *et al.*, 2007) the ensemble of the dew point profiles was close to the temperature profiles (reduced spreading), indicating a relatively humid environment in this layer in the cases under study. The mean dewpoint deficit was 2.4 °C and the 75th percentile of the dewpoint values reached 7.0 °C in this layer. Moistening at the top of the inflow layer could have aided in the rapid growth of hailstones (Kumjian *et al.*, 2021). In the mid-troposphere, the ensemble of profiles again exhibited greater spread, with cases where a strong mid-level drying characterized the environment (mean dewpoint deficit = 10.9 °C, and the 75th percentile of the dewpoint deficit = 16.3 °C at 500 hPa). So, large hail

formed by rather varied moisture and CAPE profiles, very similarly to the results found by *Nixon et al.* (2023). Furthermore, mid-level dryness – if it is not too large to suppress convection - can enhance downdraft, which will create stronger cold pools, thus increasing secondary convection and formation of more graupel particles that can affect hail formation (*Miao and Yang, 2022*).

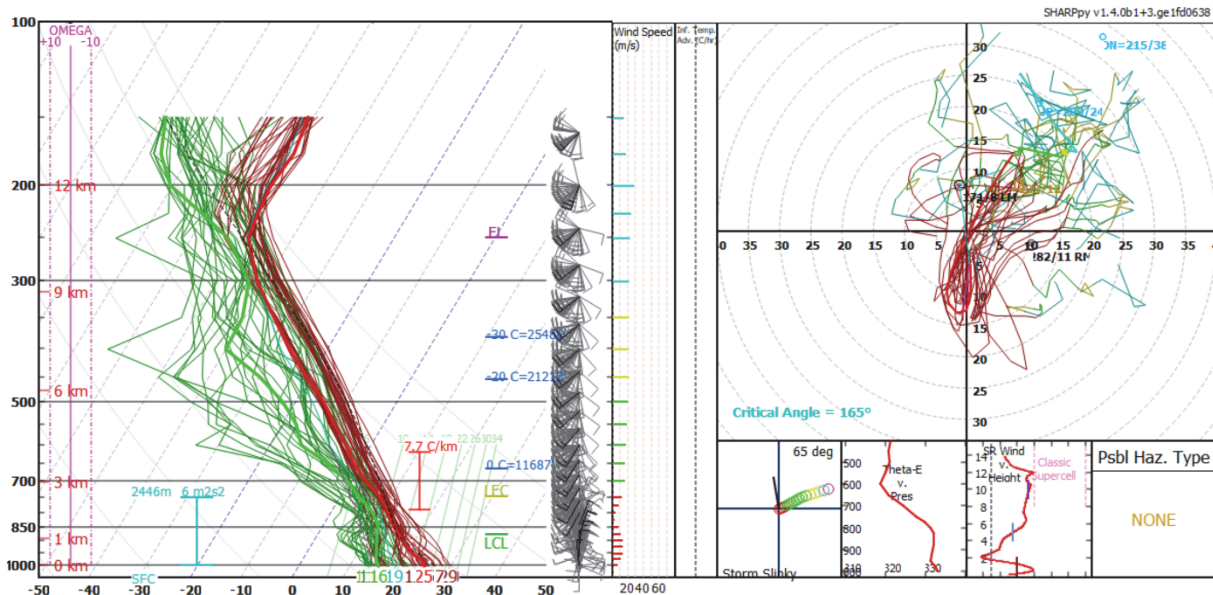


Fig. 1. Ensemble sounding and hodograph based on large hail cases between 2018 and 2023 in Hungary. On the thermodynamic diagram (left panel), the red lines indicate the temperature profiles and the green lines depict the dew point profile. The colors of the hodograph sections represent different layers (red: 0–3 km; green: 3–6 km; yellow: 6–9 km; cyan: 9–15 km). The bold lines represent the first date of the dataset. For the interpretation of the insets, see the help (*Blumberg et al., 2017*).

Examining the ensemble hodograph, we found that northerly winds dominated in the near-surface layer (as shown in the skew-T diagrams), and then the wind quickly veered (turned counterclockwise) within the lowest 1 km layer, followed by typically straight hodograph shape in the upper levels. To further analyze the hodographs, we created a composite storm-relative hodograph representing the 75th percentile of the u and v components of the datasets at each given level. The results are discussed in the following section.

3.2. Composite hodograph

The shape of the obtained storm-relative composite hodograph exhibits similarities with hodographs presented in previous studies (*Nixon and Allen, 2022; Kumjian et al., 2023; Púčik et al., 2023*) (*Fig. 2*). The main similarity lies in the weaker 0–1 km wind shear (based on the presented articles, strong wind shear in the 0–1 km layer is more typical of tornado cases), as well as the elongated and

relatively straight hodograph observed especially between 1 and 3 km. However, it is interesting to note that a dominant northerly wind component appears below 500 m, which quickly veers with height within the inflow layer. The vorticity induced by wind shear in this layer is relatively large and streamwise for right-moving supercells (500 m mean streamwise vorticity = 0.009 s^{-1}). Therefore, this sharp wind shift could provide the necessary helical updrafts in the inflow layer, which could be important for supercells producing large hail. It remains unclear from the results whether a northerly wind component near the surface is a necessary criterion. In this layer, a relatively high ($\sim 15 \text{ ms}^{-1}$) storm-relative inflow was apparent, which facilitated the development of wide updrafts (Peters *et al.*, 2019; 2020). However, storm-relative winds decreased with height, and weak storm-relative winds were observed in the hail growth zone. Despite the low number of cases, characteristics that appeared on the composite hodograph are corroborated by the results of the aforementioned previous studies.

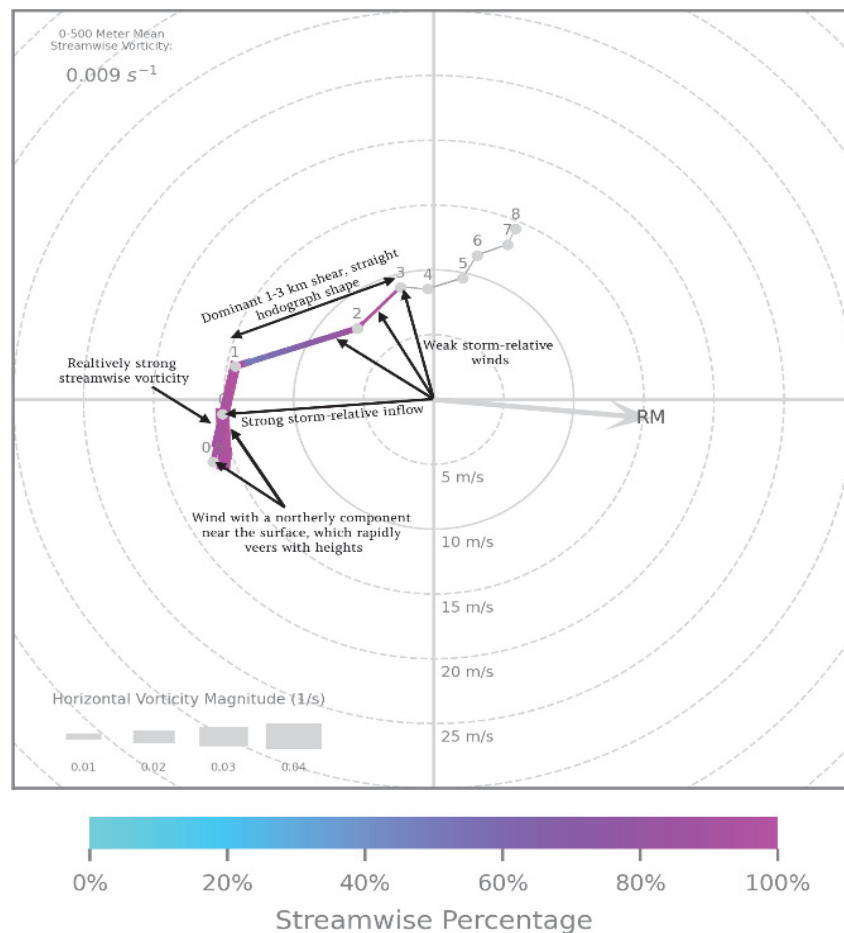


Fig. 2. Composite storm-relative hodograph created from the 75th percentile of the u and v components of each given level. The thickness of the hodograph represents the horizontal vorticity magnitude generated by the vertical wind shear, and the colors depict the streamwiseness of the horizontal vorticity relative to the inflow. The gray arrow represents the original storm motion for the right-moving (RM) supercell.

3.3. Archive case of 12 June 2018

Radiosondes are launched at 0000 and 1200 UTC every day. In Hungary, the launches take place in Budapest and Szeged (situated 170 km distance apart), making it very difficult to validate the conclusions drawn from reanalysis with measurement data. In the absence of proper proximity soundings, we present some cases from the period preceding the start of the NAK data collection period (i.e., before 2019), where large hail was reported by eyewitnesses, and nearby ERA5 soundings and hodographs are presented, generated by the rawinsonde.com website from the grid points closest to the observation location.

On June 12, 2018, an elongated frontal zone approached the Carpathian Basin from the west, with a warm, moist, unstable air mass accumulating in the warm sector. The most favorable conditions for thunderstorm development were primarily in the northwestern and northeastern thirds of the country. A small cluster of thunderstorms reached the Hungarian border from Austria at 1200 UTC (*Fig. 3a*), with its outflow gradually spreading southward and southeastward (*Fig. 3b*). Along the outflow boundary at 1430 UTC, new storms initiated (*Fig. 3c*), and developed into supercells as they moved along the boundary (*Fig. 3d*).

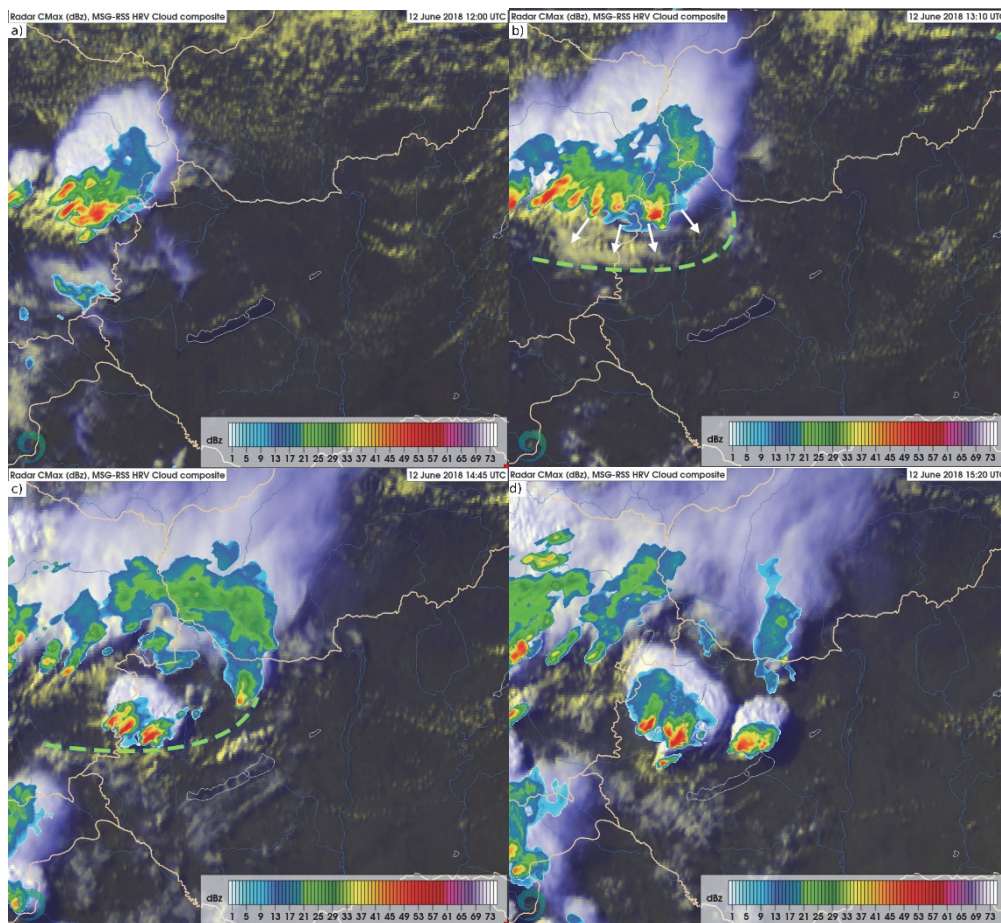


Fig. 3. The outflow boundary (dashed green line) initiated new supercells (depicted by column maximum radar reflectivity field) overlaid on visible spectrum satellite images on 12 June 2018 between 1200 and 1520 UTC (a–d). The white arrows represent the outflow motion of the boundary.

Due to the outflow boundary, northern winds dominated near the surface, but this was limited only to a shallow layer. The wind profile quickly veered due to warm air advection, and we found a relatively straight, elongated hodograph shape, especially in the 1–3 km layer (*Fig. 4*). The characteristics consistent with the above-mentioned results (*Fig. 1*) are evident in both the thermodynamic profile and the hodograph. Namely: a dry layer near the surface, moistening at the top of the inflow layer, mid-level dry conditions, a significant portion of CAPE located below the -10 °C layer, northerly and veering winds near the surface, strong (~15 ms⁻¹) storm-relative inflow, streamwise vorticity in the inflow layer, relatively straight hodograph, and small storm-relative winds in the hail growth zone (approximately the -10 °C to -30 °C layer).

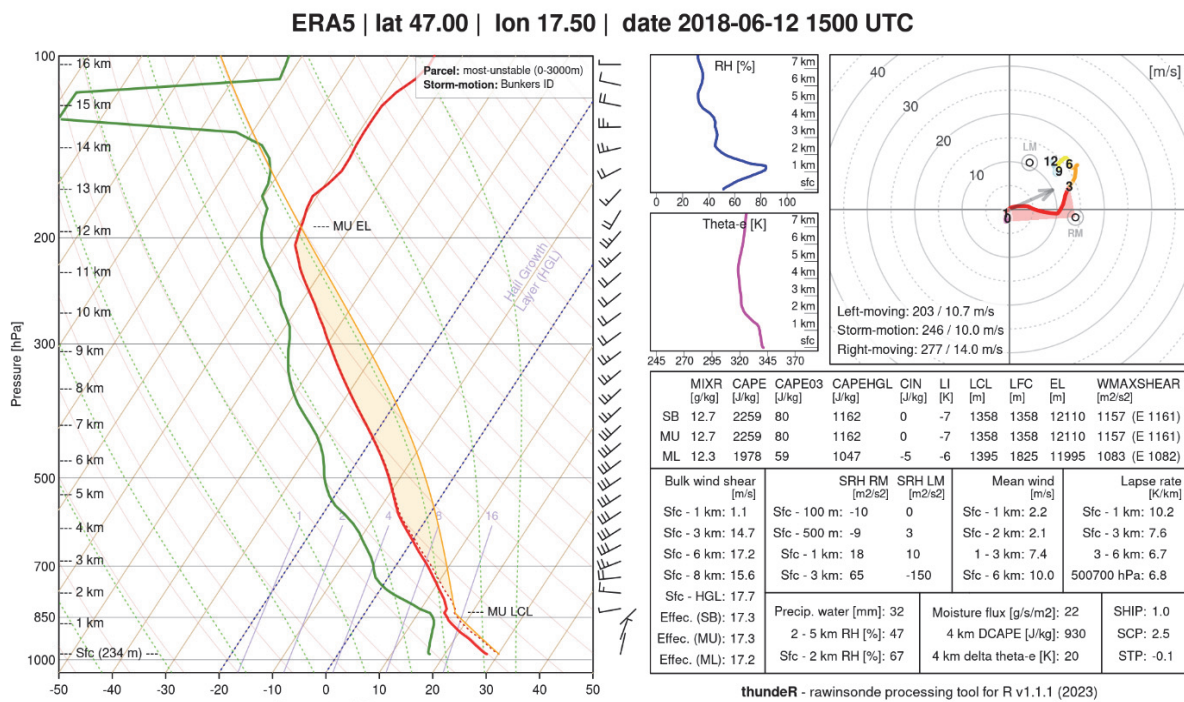


Fig. 4. ERA5 sounding and hodograph for June 12, 2018, at 1500 UTC generated by rawinsonde.com webpage. The red line on the left panel represents the environmental temperature profile, and the green line depicts the dew point profile. The yellow shaded area represents the total amount of potential energy available to the most unstable air parcel. The wind barbs show the environmental wind at each given level. The colors of the hodograph (right top panel) represent different layers (purple: 0–1 km; red: 1–3 km; orange: 3–6 km; yellow: 6–9 km; cyan: 9–12 km). The gray arrow depicts the mean motion vector, the empty circles represent the motion direction for right-mover (RM) and left-mover (LM) supercells. For the interpretation of the insets, see the help on the rawinsonde.com webpage.

Based on observations, large hail was also reported in Ajka (Veszprém county) on the Köpönyeg.hu Facebook page [3 – Köpönyeg.hu] produced by a supercell (*Fig. 5*). According to the ESSL (European Severe Storms Laboratory) observation guide [4 – ESSL], the largest hailstone could have reached a diameter of 4–5 cm.



Fig. 5. Large hail observation from a supercell on June 12, 2018 around 1600 UTC.

4. Conclusion

In this study, we examined thunderstorms that produced large hail. We investigated the environmental characteristics of the storms using ERA5 data and attempted to find similarities in the thermodynamic and kinematic characteristics of each case. Based on the ensemble diagrams (*Fig. 1*) and the hodograph created from the 75th percentile of the dataset (*Fig. 2*), we found the following characteristics in the environment of thunderstorms producing large hail:

- Large hail can form by various moisture profiles, and a considerable portion of the cases is characterized by mid-level dryness and an inverted V profile near the ground (high cloud base) with an average 6.3 °C dew point deficit.

The 75th percentile of the dew point deficit was 9.4 °C, and the 25th percentile of the dewpoint deficit was 3.1 °C near the surface.

- A significant portion (~60%, similar to *Půček et al.*, 2023b) of CAPE is generated below the -10°C layer (more than 50% of the cases).
- Strong storm-relative inflow (~15 ms⁻¹) near the surface (more than 60% of the cases).
- Sufficiently large (>15 m/s) 0–6 km vertical wind shear (more than 80% of the cases).
- Typically northerly winds near the surface, which quickly veer in the lowest 1 km (more than 50% of the cases)
- Strong streamwise environmental vorticity in the lowest 500 m (mean streamwise vorticity = 0.009 s⁻¹)
- Straight 1–3 km hodograph profile, weak winds at the top of the inflow layer relative to the storm (more than 80% of the cases).

However, these conclusions were based on a small number of cases, and although most of the results can be supported by previous studies, significantly more data would be needed to strengthen these results. It must be further emphasized that there can be cases where not all the conditions have to be fulfilled for large hail formation, as the cases were specifically selected when damaging hail occurred. Although the aforementioned criteria can be good indicators for their timely recognition, thus aiding the public warning system.

The ERA5 data only allowed the examination of environmental kinematic and thermodynamic characteristics, however, the authors would like to emphasize that cloud microphysical processes and PBL characteristics also play an important role in the formation of large hail. Our future plans include a comparison of the results of large hail events with those cases where only smaller hailstones were observed. In addition, it may be worthwhile to expand the dataset with cherry-sized hail (>2 cm) detections, thus a larger data set would be available to determine stronger results. Furthermore, it is worth noting upon the case of 12 June 2018, that small-scale processes or weather objects (in that specific case: an outflow boundary) can also contribute to the intensification of thunderstorms. These processes may not necessarily appear in NWP model forecasts and especially not in reanalyses and thus are not visible in the preliminary environment either.

Acknowledgments: The authors are grateful to the HungaroMet Hungarian Meteorological Service for making the data available for research. We are also grateful to our colleague András Imre Vaszkó for assistance in exploring archival cases. Hajnalka Breuer was supported by the Hungarian Scientific Research Fund under the grant FK132014. The research was supported by the DIMOP_PLUSZ-2.3.1-23-2023-00001 "Developing an environmental monitoring system using installed data collection network and creating a climate data repository with associated service environment" Project, implemented by HungaroMet Hungarian Meteorological Service.

References

- Allen, J.T., Giammanco, I.M., Kumjian, M.R., Punge, H.J., Zhang, Q., Groenemeijer P., Kunz, M., and Ortega, K., 2020: Understanding hail in the Earth system. *Rev. Geophys.* 58, e2019RG000665. <https://doi.org/10.1029/2019RG000665>
- Battaglioli, F., Groenemeijer, P., Púčík, T., Taszarek, M., Ulbrich, U., and Rust, H., 2023: Modeled Multidecadal Trends of Lightning and (Very) Large Hail in Europe and North America (1950–2021). *J. Appl. Meteorol. Clim.* 62, 1627–1653. <https://doi.org/10.1175/JAMC-D-22-0195.1>
- Blumberg, W.G., Halbert, K.T., Supinie, T.A., Marsh, P.T., Thompson, R.L., and Hart, J.A., 2017: SHARPPy: An Open-Source Sounding Analysis Toolkit for the Atmospheric Sciences, *Bulletin of the American Meteorological Society*, 98(8), 1625–1636. <https://doi.org/10.1175/BAMS-D-15-00309.1>
- Changnon, S., Changnon, D., and Hilberg, S.D., 2009: Hailstorms across the nation: An atlas about hail and its damages. *Illinois State Water Survey Contract Rep. 2009(12)*, 92.
- Coffer, B.E., Taszarek, M., and Parker, M.D., 2020: Near-Ground Wind Profiles of Tornadoic and Nontornadoic Environments in the United States and Europe from ERA5 Reanalyses. *Wea. Forecast.* 35, 2621–2638. <https://doi.org/10.1175/WAF-D-20-0153.1>
- Csirmaz, K., 2015: A new hail size forecasting technique by using numerical modeling of hailstorms: A case study in Hungary. *Időjárás* 119, 443–474.
- Dennis, E.J. and Kumjian, M.R., 2017: The impact of vertical wind shear on hail growth in simulated supercells. *J. Atmos. Sci.* 74, 641–663. <https://doi.org/10.1175/JAS-D-16-0066.1>
- Horváth, Á. and Geresdi, I., 2001: Severe convective storms and associated phenomena in Hungary. *Atmos. Res.* 56, 127–146. [https://doi.org/10.1016/S0169-8095\(00\)00094-6](https://doi.org/10.1016/S0169-8095(00)00094-6)
- Horváth, Á. and Geresdi, I., 2003: Severe storms and nowcasting in the Carpathian basin. *Atmos. Res.* 67–68, 319–332. [https://doi.org/10.1016/S0169-8095\(03\)00065-6](https://doi.org/10.1016/S0169-8095(03)00065-6)
- Horváth, Á., Geresdi, I., and Csirmaz, K., 2006: Numerical simulation of a tornado producing thunderstorm: a case study. *Időjárás* 110, 279–297.
- Horváth, Á., Geresdi, I., Németh, P., Csirmaz, K., and Dombai, F., 2009: Numerical modeling of severe convective storms occurring in the Carpathian Basin. *Atmos. Res.* 93, 221–237. [10.1016/j.atmosres.2008.10.019](https://doi.org/10.1016/j.atmosres.2008.10.019)
- Komjáti, K., Csirmaz, K., Breuer, H., Kurcsics, M., and Horváth, Á., 2023: Supercell interactions with surface baroclinic zones in the Carpathian Basin, 11th European Conference on Severe Storms, Bucharest, Romania, 8–12 May 2023, ECSS2023-39. <https://doi.org/10.5194/ecss2023-39>
- Kumjian, M.R. and Lombardo, K., 2020: A hail growth trajectory model for exploring the environmental controls on hail size: Model physics and idealized tests. *J. Atmos. Sci.* 77, 2765–2791. <https://doi.org/10.1175/JAS-D-20-0016.1>
- Kumjian, M.R., Lombardo, K., and Loeffler, S., 2021: The evolution of hail production in simulated supercell storms. *J. Atmos. Sci.* 78, 3417–3440. <https://doi.org/10.1175/JAS-D-21-0034.1>
- Kumjian, M., Lombardo, K., Nixon, C., and Allen, J., 2023: Does Low-level Vertical Wind Shear Matter for Hail Production? 11th European Conference on Severe Storms, Bucharest, Romania, 8–12 May 2023, ECSS2023-91. <https://doi.org/10.5194/ecss2023-91>
- Li, F., Chavas, D.R., Reed, K.A., and Dawson II, D.T., 2020: Climatology of Severe Local Storm Environments and Synoptic-Scale Features over North America in ERA5 Reanalysis and CAM6 Simulation. *J. Climat.* 33, 8339–8365. <https://doi.org/10.1175/JCLI-D-19-0986.1>
- Maddox, R.A., Hoxit, L.R., and Chappell, C.F., 1980: A study of tornadoic thunderstorm interactions with thermal boundaries. *Mon. Weather Rev.* 108, 322–336. [https://dx.doi.org/doi:10.1175/1520-0493\(1980\)108%3C0322:ASOTTI%3E2.0.CO;2](https://dx.doi.org/doi:10.1175/1520-0493(1980)108%3C0322:ASOTTI%3E2.0.CO;2)
- Magee, K.M. and Davenport, C.E., 2020: An observational analysis quantifying the distance of supercell-boundary interactions in the great plains. *J. Operat. Meteor.* 8(2), 15–38, <https://doi.org/10.15191/nwajom.2020.0802>
- Markowski, P.M., Rasmussen, E.N., and Straka, J.M., 1998: The occurrence of tornadoes in supercells interacting with boundaries during VORTEX-95. *Wea. Forecasting* 13, 852–859. [https://doi.org/10.1175/1520-0434\(1998\)013%3C0852:TOOTIS%3E2.0.CO;2](https://doi.org/10.1175/1520-0434(1998)013%3C0852:TOOTIS%3E2.0.CO;2)

- Martius, O., Hering, A., Kunz, M., Manzato, A., Mohr, S., Nisi, L., and Trefalt, S., 2018: Challenges and recent advances in hail research. *Bull. Amer. Meteorol. Soc.*, 99, ES51–ES54. <https://doi.org/10.1175/BAMS-D-17-0207.1>
- Miao, J. and Yang, M., 2022: The impacts of mid-level moisture on the structure, evolution and precipitation of afternoon thunderstorms: A real-case modeling study at Taipei on 14 June 2015. *J. Atmos. Sci.* 98, 129–152. <https://doi.org/10.1175/JAS-D-21-0257.1>
- Mulholland, J.P., Peters, J.M., and Morrison, H., 2021: How Does LCL Height Influence Deep Convective Updraft Width? *Geophys. Res. Lett.* 48, e2021GL093316. <https://doi.org/10.1029/2021GL093316>
- Nixon, C.J. and Allen, J.T., 2022: Distinguishing between hodographs of severe hail and tornadoes. *Wea. Forecasting* 37, 1761–1782. <https://doi.org/10.1175/WAF-D-21-0136.1>
- Nixon, C.J., Allen, J.T., and Taszarek, M., 2023: Hodographs and Skew Ts of Hail-Producing Storms. *Wea. Forecasting* 38, 2217–2236. <https://doi.org/10.1175/WAF-D-23-0031.1>
- Peters, J.M., Nowotarski, C.J., and Morrison, H., 2019: The role of vertical wind shear in modulating maximum supercell updraft velocities. *J. Atmos. Sci.*, 76, 3169–3189. <https://doi.org/10.1175/JAS-D-19-0096.1>
- Peters, J.M., Nowotarski, C.J., Mulholland, J.P., and Thompson, R.L., 2020: The influences of effective inflow layer streamwise vorticity and storm-relative flow on supercell updraft properties. *J. Atmos. Sci.* 77, 3033–3057, <https://doi.org/10.1175/JAS-D-19-0355.1>
- Piasecki, K., Matczak, P., Taszarek, M., Czernecki, B., Skop, F., and Sobisiak, A., 2023: Giant hail in Poland produced by a supercell merger in extreme instability – A sign of a warming climate? *Atmos. Res.* 292. <https://doi.org/10.1016/j.atmosres.2023.106843>
- Púčik, T., Castellano, C., Groenemeijer, P., Kühne, T., Rädler, A. T., Antonescu, B., and Faust, E., 2019: Large hail incidence and its economic and societal impacts across Europe. *Mon. Weather Rev.* 147, 3901–3916. <https://doi.org/10.1175/MWR-D-19-0204.1>
- Púčik, T., Groenemeijer, P., Singer, M., Ryva, D., Stanek, M., Pistotnik, G., Kaltenberger, R., and Holzer, A., 2023a: Damage survey, environment and storm-scale evolution of the giant hail and F4 tornado producing supercell on 24 June 2021, 11th European Conference on Severe Storms, Bucharest, Romania, 8–12 May 2023, ECSS2023-143. <https://doi.org/10.5194/ecss2023-143>
- Púčik, T., Groenemeijer, P., Taszarek, M., and Battaglioli, F., 2023b: Pre-storm environments and storm-scale properties of the major hailstorms of 2021 and 2022 in Europe., 11th European Conference on Severe Storms, Bucharest, Romania, 8–12 May 2023, ECSS2023-124. <https://doi.org/10.5194/ecss2023-124>
- Raupach, T.H., Martius, O., Allen, J.T., Kunz, M., Lasher-Trapp, S., Mohr, S., Rasmussen, K.L., Trapp, R.J., and Zhang, Q., 2021: The effects of climate change on hailstorms. *Nat. Rev. Earth Environ.* 2, 213–226. <http://dx.doi.org/10.1038/s43017-020-00133-9>
- Taszarek, M., Allen, J.T., Púčik, T., Hoogewind, K.A., and Brooks, H.E., 2020: Severe Convective Storms across Europe and the United States. Part II: ERA5 Environments Associated with Lightning, Large Hail, Severe Wind, and Tornadoes. *J. Climat.* 33, 10263–10286. <https://doi.org/10.1175/JCLI-D-20-0346.1>
- Taszarek, M., Pilguy, N., Allen, J.T., Gensini, V., Brooks, H.E., and Szuster, P., 2021: Comparison of Convective Parameters Derived from ERA5 and MERRA-2 with Rawinsonde Data over Europe and North America. *J. Climat.* 34, 3211–3237. <http://dx.doi.org/10.1175/JCLI-D-20-0484.1>
- Taszarek, M., Allen, J., Nixon, C., Dowdy, A., and Battaglioli, F., 2023a: Do severe storms across Australia, Europe and the United States share similarities? A comparison of atmospheric profiles and environmental predictors, 11th European Conference on Severe Storms, Bucharest, Romania, 8–12 May 2023, ECSS2023-25. <https://doi.org/10.5194/ecss2023-25>
- Taszarek, M., Czernecki, B., and Szuster, P., 2023b: thundeR - a rawinsonde package for processing convective parameters and visualizing atmospheric profiles, 11th European Conference on Severe Storms, Bucharest, Romania, 8–12 May 2023, ECSS2023-28. <https://doi.org/10.5194/ecss2023-28>
- Thompson, R.L., Mead, C.M., and Edwards, R., 2007: Effective storm-relative helicity and bulk shear in supercell thunderstorm environments. *Wea. Forecasting* 22, 102–115. <https://doi.org/10.1175/WAF969.1>

Wurman, J., Richardson, Y., Alexander, C., Weygandt, S., and Zhang, P.F., 2007: Dual-Doppler and single-Doppler analysis of a tornadic storm undergoing mergers and repeated tornadogenesis. *Mon. Weather Rev.* 135, 736–758, <https://doi.org/10.1175/MWR3276.1>

Online sources:

[1 – GitHub] <https://github.com/SamBrandtMeteo/Storm-Relative-Hodograph-Plotter>

[2 – Rawinsonde] http://rawinsonde.com/ERA5_Europe/

[3 – Köpönyeg.hu]

<https://www.facebook.com/photo/?fbid=10156507851324312&set=a.473986179311>

[4 – ESSL] https://www.essl.org/cms/wp-content/uploads/ESSL_hail_size_comparisons.pdf

Appendix

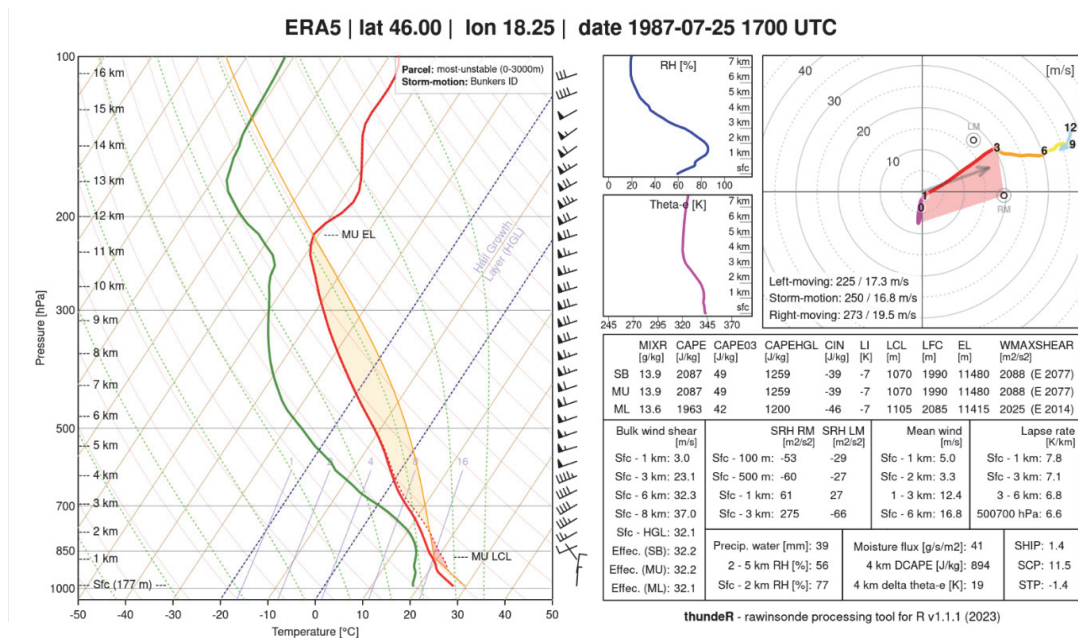


Fig. A1. Same as Fig. 4, but at 1700 UTC on July 25, 1987.

ERA5 | lat 48.25 | lon 22.25 | date 2009-06-07 1700 UTC

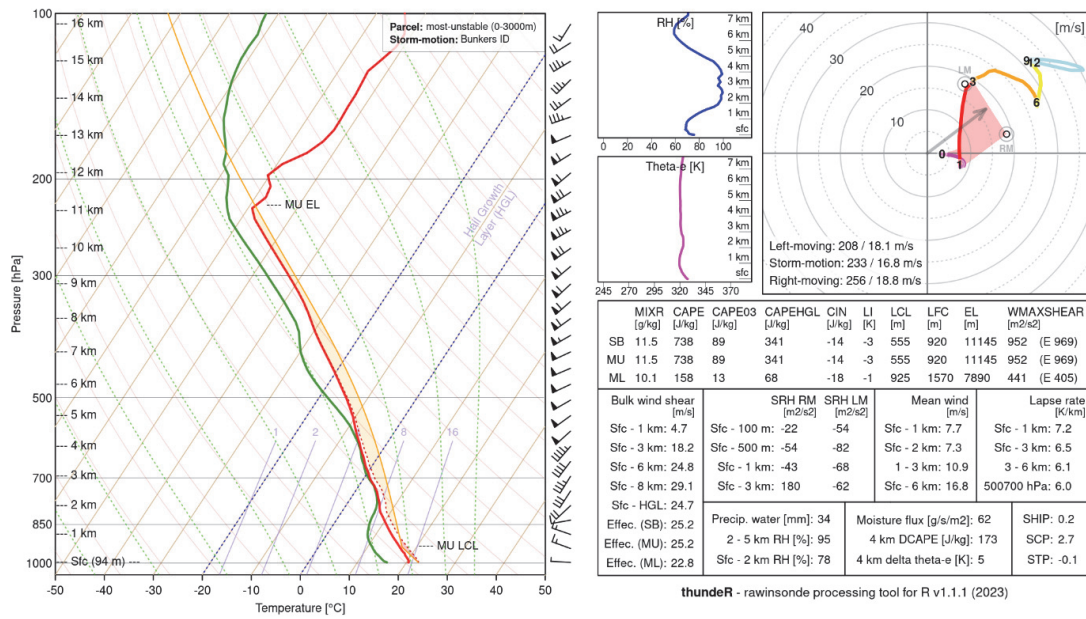


Fig. A2. Same as Fig. 4, but at 1700 UTC on June 7, 2009.

ERA5 | lat 46.00 | lon 18.25 | date 2009-06-16 1700 UTC

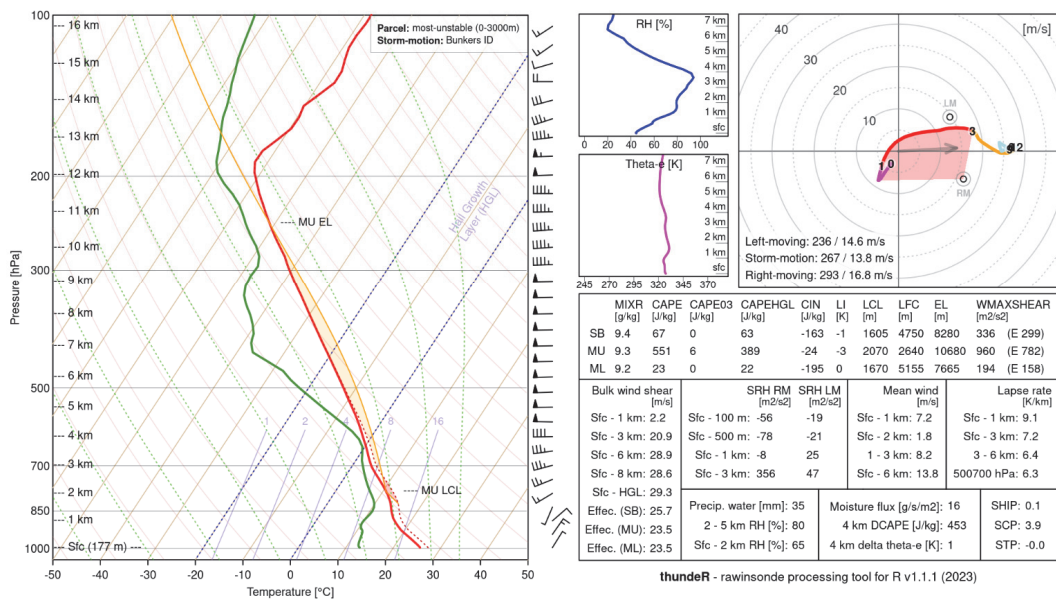


Fig. A3. Same as Fig. 4, but at 1700 UTC on June 16, 2009.

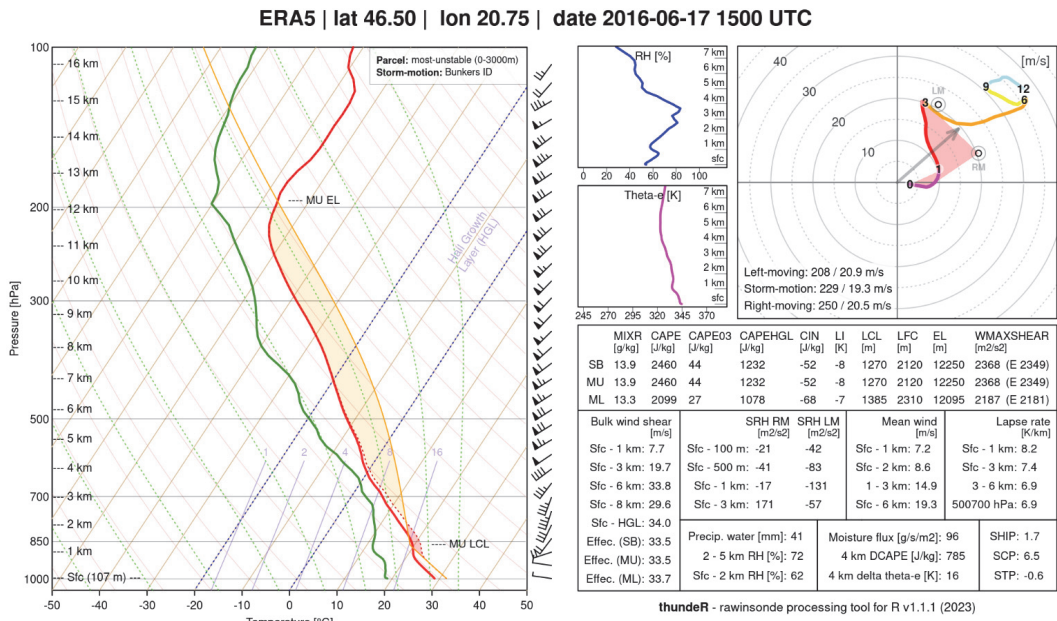


Fig. A4. Same as Fig. 4, but at 1500 UTC on June 17, 2016.

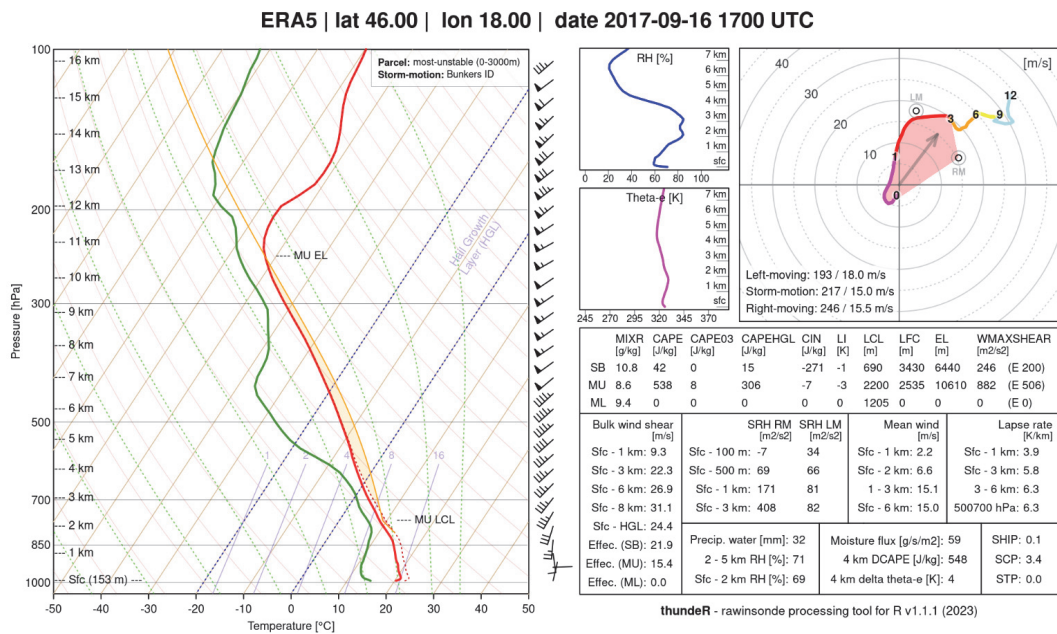


Fig. A5. Same as Fig. 4, but at 1700 UTC on September 16, 2017.